

NUMERICAL SIMULATION OF AIRFOILS APPLIED TO UAVs

Paulo Cézar Pereira Corrêa, paulocpcorreia@outlook.com

University of Brasilia - UnB

Manuel Nascimento Dias Barcelos Júnior, manuelbarcelos@gmail.com

University of Brasilia – UnB at Gama

Abstract. *This essay aims the process optimization when referred to aeronautical projects. By using mesh generators softwares and simulations made in CFD, the article employs numerical techniques to simulate airfoils and shows that is possible to extract accurated and conservative outcomes when compared to wind tunnel results. The test cases studied were based on the Selig 1223 type of airfoil and developed into the ANSYS platform, whereas by using the ICEM mesh tool, structured meshes were generated and imported to the CFX enviroment, where they could be simulated and analyzed.*

Keywords: Airfoils, CFX, ICEM, Selig 1223

1. NOMENCLATURE

u	velocity
p	pressure
u'	speed fluctuation
k	turbulent kinetic energy
I	tensor identity
S	strain rate tensor
L	lift
F_x	horizontal force
F_y	vertical force
C_l	lift coeficiente
A_x	horizontal projection of the airfoils surface

Greek Symbols

α	angle of attack
ρ	specific mass
τ	viscous stress tensor
μ	viscosity
μ_t	turbulent viscosity
μ_{eff}	effective viscosity

Subscripts

max	maximum
min	minimum
—	Average operator

2. INTRODUCTION

The UAV, unmanned aerial vehicle, is an aircraft that creates the needed lift to the flight by means of aerodynamic forces. The presence of pilots is not required, and it can also be radio-controlled with the need or not of human supervision, if its operation is fully automatic, the application of Programmable Logical Controlers (PLC) is necessary.

The concept of light, cheap, small, unmanned aircraft was first idealized for military purposes and has been gaining ground since I World War. In Brazil, its uses were evident in the last decade, when the civil purpose of recognizing and monitoring great areas became important for security reasons (Maj. Christopher, 1997).

Nowadays, in Brazil, the UAV has several different applications, which benefits by the association between enterprises and universities that provide fully national developed technologies.

The project missions are nothing more than objectives to be achieved that define the aircraft, which can be military or civilian. The work applications range from areas such as attack and rescue to monitoring and transportation.

Given the importance of UAV's for technological development, civilian or military, this article aims to facilitate the process of aircraft design.

The design of the entire aircraft is complex, and it's subdivided into smaller sets such as Aerodynamics, Structure, Stability and Propulsion. Depending on the kind of operation of the vehicle, it is understandable that the aerodynamic design area has a degree of considerable importance, with the main task of selecting airfoils to be used on the wing and control surfaces.

The choice of shape to be used is based on its aerodynamic characteristics, namely: the amount of lift, the drag produced, and the momentum generated by it. The most conventional way to analyze these characteristics is through wind tunnel tests, a process extremely reliable, but with a high cost associated when dealing with small projects. Besides being an experimental procedure which requires data to be collected out over many trials, it is also necessary skilled labor and high cost equipment.

It is worth emphasizing that the wing design aimed, here, in this work has a wingspan of 3 meters and a root cord of 0.3 meters or so. Therefore, a wind tunnel capable of supporting a full size aerodynamic surface is difficult to build and

too expensive to justify to fulfill the project requirements.

The implementation of a validated computational analysis can result in a faster and cheaper aerodynamic design without sacrificing reliability. The CFD, English short for Computational Fluid Dynamics, is nothing more than a numerical tool to analyze fluid-dynamic systems. This tool is based on the computational solution of the equations of mass, momentum and energy conservation that govern the flow.

The methodology to implement a CFD approach in the design framework consists of several steps. Primarily, it is performed the study and the development of the mesh to computationally represent the fluid using the platform ICEM-CFD. The construction of the mesh over the aerodynamic surface guarantying the quality of mesh elements ensures a realistic flow representation.

Next, it is defined the boundary conditions of the problem. They are basically related to the flow characteristics, if incompressible or compressible, if inviscid or viscous and if laminar or turbulent. Finally, the test cases are solved and the computer generated outcomes are post-processed by extracting the properties of interest on the aerodynamic surfaces. The test cases were based on the Selig 1223 airfoil geometry, because it is a shape with a wide experimental study available, what facilitates the comparison of results. The Reynolds number used in the simulations is about 300,000. In addition, comparisons of different turbulence models are executed in order to obtain the one that best approximates the experimental results, thus, bringing greater reliability to the process of computational analysis.

3. THEORY

3.1 Reynolds-averaged Navier–Stokes equations

The determination of the pressure and velocity fields is done by the two transport equations, the mass conservation equation and the momentum equation. But as all turbulent flow is tridimensional and transient, the equations take a high computational cost to be solved considering the present scales, making it necessary to simplify them using algorithms, as in the turbulence models based on the Reynolds-Averaged (RANS).

The turbulence models based on the Reynolds-Average follow a methodology called (RANS), in which is proposed that instead of trying to predict the temporal evolution of the flow, an average calculus would be done on the Navier–Stokes equations.

$$\nabla \cdot (\rho \mathbf{u}) = 0 \quad (1)$$

$$\frac{\partial(\rho \mathbf{u})}{\partial t} + \nabla \cdot (\rho \mathbf{u} \mathbf{u}) = -\nabla p + \nabla \cdot \tau - \nabla \cdot \overline{\rho \mathbf{u}' \mathbf{u}'} \quad (2)$$

The last term of the equation (2) represents the Reynolds tensor. In the CFX software modeling, the Reynolds tensor is calculated by a linear model based on the diffusion gradient hypothesis, in other words, the Boussinesq hypothesis.

3.2 Linear model (Boussinesq Hypothesis)

This linear and isotropic model is the oldest one used to represent the Reynolds tensor. It is based on the Boussinesq Hypothesis (1887), which defines that the Reynolds tensions are proportional to the average velocity gradient, and its representations is given by:

$$-\overline{\rho \mathbf{u}' \mathbf{u}'} = \frac{2}{3} \rho k \mathbf{I} - 2\mu_t \mathbf{S} \quad (3)$$

Besides the constitutive equation necessary to define the Reynolds tensor, it is also necessary the use of a turbulence model to calculate the length scales and the turbulence velocity. The models used in this work, were the k-epsilon and the SST k-omega.

3.3 k-epsilon model

The two equations turbulence model, standard k-epsilon, in which the velocity and the length scale are solved using separated transport equations, is widely used in the turbulence determination, because it offers a good balance between numeric effort and computational accuracy.

The turbulent viscosity is defined in this model as the product of a turbulent velocity and a length scale. In this kind of arrangement, the turbulent velocity scale is derived from the turbulent kinetic energy provided from the solution of its transport equation.

The length scale is estimated by two properties of the turbulence field, generally the turbulence kinetic energy and its dissipation rate. The turbulence kinetic – k – is defined as the variation on the velocity fluctuation. The turbulent

dissipation of the swirl – ε – is defined as the rate in which velocity fluctuations dissipate and have the dimension k by time unity ($L \cdot t^{-3}$), for example $m \cdot s^{-3}$.

$$\mu_{eff} = \mu + \mu_t \quad (4)$$

The k-epsilon model assumes that the turbulent viscosity is associated to the turbulence kinetic energy by the expression:

$$\mu_t = C_\mu \rho \frac{k^2}{\varepsilon} \quad (5)$$

In which C_μ is a Constant.

The k and ε values are obtained directly from the transport differential equations of turbulent kinetic energy and the turbulent dissipation rate.

$$\frac{\partial(\rho k)}{\partial t} + \frac{\partial(\rho u_j k)}{\partial x_j} = \frac{\partial}{\partial x_j} \left[\left(\mu + \frac{\mu_t}{\sigma_k} \right) \frac{\partial k}{\partial x_j} \right] + P_k + P_{kt} - \rho \varepsilon \quad (6)$$

$$\frac{\partial(\rho \varepsilon)}{\partial t} + \frac{\partial(\rho u_j \varepsilon)}{\partial x_j} = \frac{\partial}{\partial x_j} \left[\left(\mu + \frac{\mu_t}{\sigma_\varepsilon} \right) \frac{\partial \varepsilon}{\partial x_j} \right] + \frac{\varepsilon}{k} (C_{\varepsilon 1} (P_k + P_{\varepsilon t}) - C_{\varepsilon 2} \rho \varepsilon) \quad (7)$$

Where ε is the kinetic energy dissipation, σ_k and σ_ε the turbulent Prandtl numbers, $C_{\varepsilon 1}$ e $C_{\varepsilon 2}$ are constants, P_{kt} and $P_{\varepsilon t}$ represent the thrust force influence, and finally P_k is the turbulence production caused by the viscous forces, which are modeled by:

$$P_k = \mu_t \nabla \mathbf{U} (\nabla \mathbf{U} + \nabla \mathbf{U}^T) - \frac{2}{3} \nabla \cdot \mathbf{U} (3\mu_t \nabla \mathbf{U} + \rho k) \quad (8)$$

The $3\mu_t$ term prevents that the k and ε constants became too big due to collisions, a situation aggravated due to the high refinement level of the mesh in the collision regions.

3.4 SST k-omega model

This Shear-Stress Transport model, SST k-omega from Menter was proposed for an aeronautic application. This turbulence model is characterized by being a hybrid model that combines the k-epsilon and k-omega equations. In practice, the SST model works as a k-omega near the walls and as k-epsilon on the further parts (Lars Davidson, 2006).

The turbulence k-omega model is in fact superior to the k-epsilon when dealing with flows on the boundary layers, in other words, flows close to the walls, even dealing with different pressure gradients cases. On the other side, for the correct use of the model, some restrictions for the boundary conditions are necessary, restrictions that the k-epsilon model does not suffer.

Therefore the SST model mixes the strong formulation of the k-omega in regions near the wall and the independence of the k-epsilon model in regions of free flow above the limit layer. Both the models are basically multiplied by a weight function and added, but for this use it is necessary to rewrite the k-epsilon equations leaving them in function of the characteristics frequency scales, ω .

The weight function given by F_1 varies according to the height of the layer analyzed, with its value in limit layer regions being zero (making k-omega predominant) and unitary in further regions (prevailing the k-epsilon model).

Finally, the turbulence kinetic energy k and the specific dissipation rate ω are defined by (Menter, 2003):

$$\frac{\partial(\rho k)}{\partial t} + \frac{\partial(\rho \bar{u}_i k)}{\partial x_i} = \frac{\partial}{\partial x_j} \left[\left(\mu + \sigma_k \mu_t \right) \frac{\partial k}{\partial x_j} \right] + \tilde{P} - \rho \beta^* k \omega \quad (9)$$

$$\frac{\partial(\rho \omega)}{\partial t} + \frac{\partial(\rho \bar{u}_i \omega)}{\partial x_i} = \frac{\partial}{\partial x_j} \left[\left(\mu + \sigma_\omega \mu_t \right) \frac{\partial \omega}{\partial x_j} \right] + \rho \alpha S^2 - \rho \beta \omega^2 + (1 - F_1) 2 \rho \sigma_d \frac{1}{\omega} \frac{\partial k}{\partial x_j} \frac{\partial \omega}{\partial x_j} \quad (10)$$

The last term of the equation above is the term relative to the crossed diffusion, it has as its main function the increase in the production of ω , and the consequent increase in the dissipation of k .

The weight function is defined as:

$$F_1 = \tanh(\arg_1^4) \quad (11)$$

Where:

$$arg_1 = \min \left[\max \left(\frac{\sqrt{k}}{\beta^* \omega y}, \frac{500\mu}{\rho y^2 \omega} \right), \frac{4\rho\sigma_\omega 2k}{CD_{k\omega} y^2} \right] \quad (12)$$

Being y the distance to the closest wall region and $CD_{k\omega}$ is the positive part of the crossed diffusion, defined by:

$$CD_{k\omega} = \max \left(2\rho\sigma_d \frac{1}{\omega} \frac{\partial k}{\partial x_j} \frac{\partial \omega}{\partial x_j}, 10^{-10} \right) \quad (13)$$

The viscosity is defined as:

$$\mu_t = \frac{a_1 k \rho}{\max(a_1 \omega, S F_2)} \quad (14)$$

Being S the module of the average shear rate, S_{ij} ,

$$S = \sqrt{2 S_{ij} S_{ij}} \quad (15)$$

$$S_{ij} = \frac{1}{2} \left(\frac{\partial \bar{u}_i}{\partial x_j} + \frac{\partial \bar{u}_j}{\partial x_i} \right) \quad (16)$$

and F_2 the mix function to the turbulent viscosity in the SST model, defined as:

$$F_2 = \tanh (arg_2^2) \quad (17)$$

$$arg_2 = \max \left(\frac{\sqrt{k}}{\beta^* \omega y}, \frac{500\mu}{\rho y^2 \omega} \right) \quad (18)$$

In the SST model, the production of turbulent kinetic energy is limited to prevent the turbulence accumulation in the stagnation region.

$$\tilde{P} = \min \left(\frac{\mu_t S^2}{\rho}, 10 \beta^* k \omega \right) \quad (19)$$

Being φ the set if necessary constants to the closure of the SST model, and φ_1 and φ_2 closure constants necessary to the k- ω and k- ϵ , respectively. The calculation of the constants has as a base the weight function as showed:

$$\varphi = F_1 \varphi_1 + (1 - F_1) \varphi_2 \quad (20)$$

Table 1. Main constants of each model.

	β	β^*	σ_k	σ_ω	σ_d	A
φ_1 (k- ω)	0.075	0.09	0.5	0.5	0.856	5/9
φ_2 (k- ϵ)	0.0828	0.09	1.0	0.856	0.856	0.44

4. NUMERICAL METHODOLOGY

The equations solved in this work are the conservation of mass, momentum and energy, also known as Navier-Stokes equations. The Navier-Stokes equations are complemented by applying a turbulence model. The whole the of equations are discretized by using a finite volume method and by a RANS methodology through several time iterations in the CFX environment.

For the modeling of the problem it was analyzed two different turbulence models to be able to trace their individual behaviors. The models were the SST and the k-epsilon.

It is difficult to compare the turbulence models directly. Due to their special features, each model responds differently to the degree of mesh refinement applied, ie, setting the ideal grid to represent the flow using the SST model is not necessarily the one which best represents the k-epsilon model. Therefore, for a fair comparison, three mesh

configurations were designed with different degrees of refinement. They were identified as Alta, Média and Baixa, with 2.665.600, 666.400 and 166.600 volume elements respectively.

The turbulence model first adapted to the Navier-Stokes equations was the Shear Stress Transport (SST), this choice was made for being a model created for the aeronautical field, enabling high fidelity in this application. The second option, the turbulence model k-epsilon, was defined by its precision in regions beyond the boundary layer, resulting in an excellent approximation since the data to be extracted for now are related to lift.

The methodology for creating the mesh was taken first by determining the geometry of the domain. To this end, it was determined a geometry in the form of "C" in which the distribution could be made as uniform as possible around the airfoil desired, Figure 1.

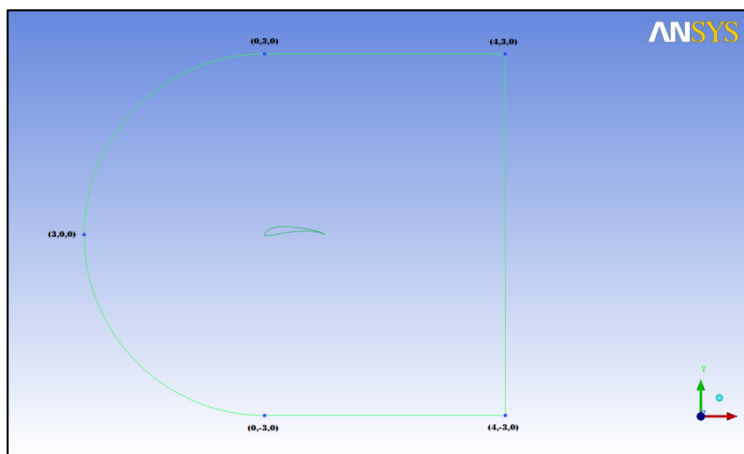


Figure 1. Problem domain

The methodology for creating the mesh, first began by determining the geometry of the domain and the way the mesh can be constructed inside. The mesh creation process consisted basically of a multiblock method, in which the domain is split into nine distinct parts which are divided into three interconnected layers, also called a central block, four internal and external blocks, Figure 2.

The central region is adapted to the geometry of the airfoil so that when it is deleted, an empty region is devised and no mesh exists there. The following internal four blocks are dimensioned to adapt to the boundary layer, and the mesh is constructed with a high level of refinement in order to model as accurate as possible the behavior near the airfoil. Finally, the external blocks are defined with a lower level of refinement.

The strategy of separating the external blocks from the internal ones close to the airfoil is chosen because this arrangement makes possible to reduce the computational cost. The separation in blocks allows the choice of different element densities for the boundary layer and the outer region. This strategy would not work if a one block mesh is created, even assuming an exponential mesh growth from the airfoil to the freestream.

At the end of the mesh generation process, the whole domain has a continuous and consistent structured mesh.

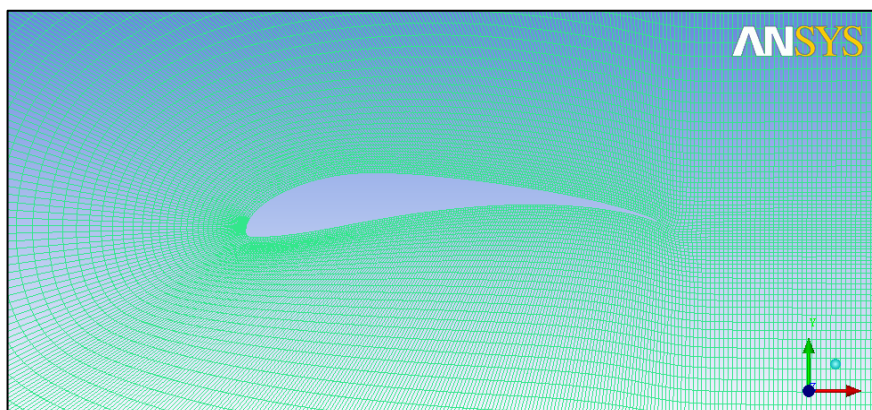


Figure 2. Mesh around the airfoil

The whole process of creating the mesh was developed with the help of the pre-processing ICFM software, and as it belongs to the ANSYS platform, the generated mesh can be saved in files with a portable format and can be used in any

numerical simulation software, not only the ones from the ANSYS package. Here, the CFX software is preferred because it is well known in the scientific and technical communities and also belongs to the ANSYS platform.

4.1 Boundary conditions

In Figure 3, it showed how the conditions were applied to the domain, and they are divided as follows: the input (Inlet) conditions defined throughout the portion of arrows directed to model, the output conditions (Outlet) defined by the portion of arrows leaving the model, the conditions at the wall defined on the body shape, and finally the symmetry conditions defined on the faces perpendicular to the z-axis.

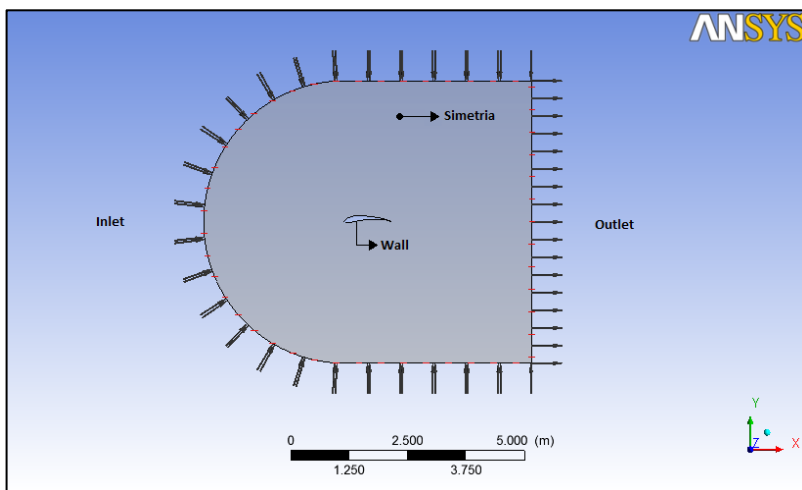


Figure 3. Representation of the boundary conditions of the airfoil

For the numerical analysis, it was assumed a turbulent, isothermal and incompressible flow, and the physical parameters were defined for air at 25°C. The simulation was also planned to truncate after the thousandth iteration or after reaching a residual value of at least 10⁻⁸.

In the turbulence models, the magnitude of the turbulence parameters were defined as an average of 0.037, as suggested by the manual of the software when simulating external flows of this sort.

5. RESULTS

As expected in the methodology, it was simulated different configurations and meshes for different angles of attack using both turbulence models.

In order to create a standard for comparison, the results were treated and arranged in curves, which represent the behavior of the lift coefficient for different angles of attack for each specific case. The curves were separated according to the turbulence model used.

5.1 Results treatment

The lift coefficient is calculated from the lift force, which was calculated with the Cartesian forces provided by CFX:

$$L = F_y \cos(\alpha) - F_x \sin(\alpha) \quad (21)$$

$$C_l = \frac{L}{\frac{1}{2} \rho V^2 A_x} \quad (22)$$

5.2 Simulations curves

The curves from Figure 4 are related to the behavior curves in the different settings applied to the k-epsilon turbulence model.

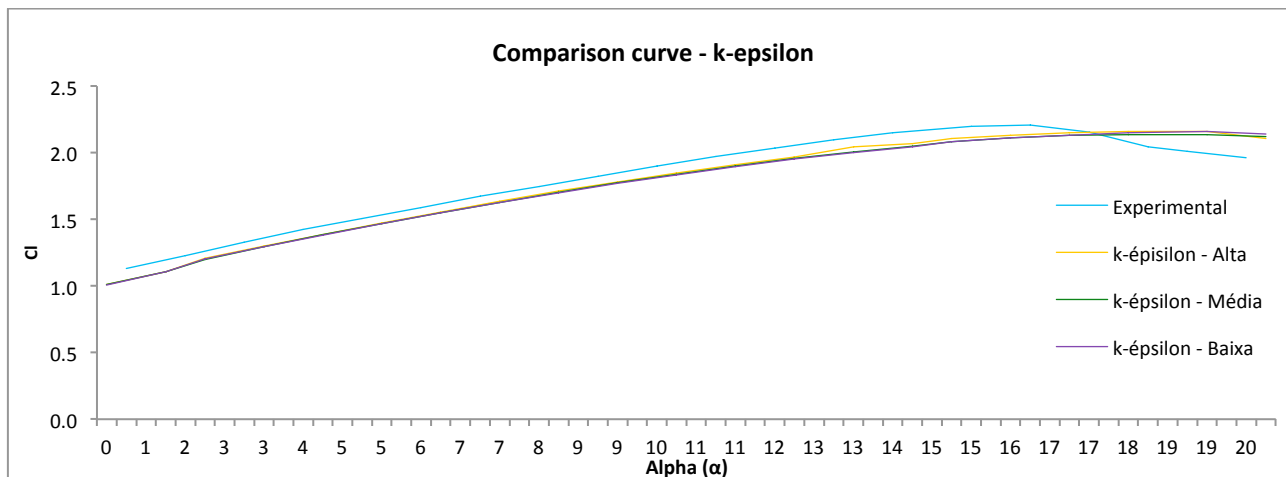


Figure 4. Comparison curve – k-epsilon

When conducting a brief analysis of the chart there are two evident characteristics of behavior, the fact of the proximity of the curves and the lack of perception of Stall. Both features observed can be easily explained by the way the modeling is done for closing the model equations. As seen in the theoretical analysis of this article, the turbulence model in question does not allow a good sensitivity in the regions near the walls; this means that the model is almost indifferent to the degree of refinement. This same cause also has as a result the lack of perception of Stall, since it is a detachment of the boundary layer around the airfoil.

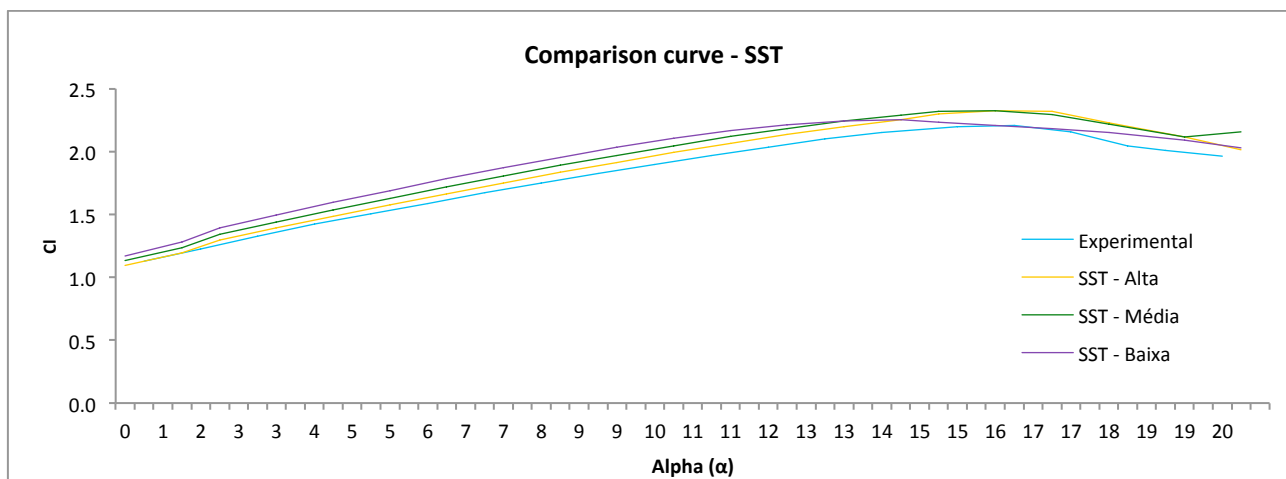


Figure 5. Comparison curve – SST

The comparison curve of the Shear Stress Transport (SST) model represented accurately its modeling of the Navier-Stokes equations, Figure 5. This is because the curves show the hybrid model characteristic as well as its commitment to the highest mesh refinement.

Observing the three simulation curves simulation, it is evident the behavior of the hybrid model. The hybrid characteristic allows us to get a good approximation of the lift coefficient observing the viscous drag on the inner boundary layer, ie, the mesh refinement in the inner regions is essential for a good result. The presence of viscous drag in the calculations also allows the perception of Stall, which can now be seen in the chart above.

It can be concluded by this article the fidelity of the presented methodology for numerical simulation, it is a good tool for developing aerodynamic projects in UAVs. Final results were precisely consistent with the proposals of each model, approaching the experimental results considerably.

The aerodynamic design of a UAV is basically to develop a wing with the best possible performance that fits the given mission. To this end, through research and theoretical foundations are selected different geometric shapes which are compared by different tools. At the end of the comparisons is chosen the setting that best suits the project.

6. CONCLUSIONS

The idea of this work is to develop a methodology to be employed as a tool of comparison for airfoils, which would reduce considerably the cost of the project, once the time and the resources spent to perform a simulation in a

computational environment are substantially lower when compared to those of a test in wind tunnel. It is clear that the methodology does not provide the same accuracy and reliability that the experimental results have, and this is not its goal. The major purpose of this work is to generate a pattern of simulations which have a minimum reliability required for making it possible to compare different airfoil geometries, in order to select the ones that best meet the project requirements. After the definition of the best set of airfoils, a few final geometries could finally be studied in wind tunnel with the aim of obtaining their most accurate characteristics, necessary for the completion of the aerodynamic design.

7. ACKNOWLEDGEMENTS

The authors would like to thank the University of Brasilia for providing the resources necessary to the research.

8. REFERENCES

- Anderson, J.D.Jr., 1984, Fundamentals of Aerodynamics, 2nded., McGraw-Hill Book Company, New York.
- Cazalbou, J.B., Sparlat, P.R., Brandshaw, P., 1993, On the Behavior of 2-Equation Models at the Edge of Turbulent Region, Physics of Fluids, Vol. 6, No. 5, pp. 1797-1804.
- Collen, D.S.P., 2004, The k-epsilon Model in the Theory of Turbulence, University of Pittsburgh, Ohio, U.S.
- Davidson, L., 2006, An Introduction to Turbulence Models. Chalmers University of Technology, Göteborg, Sweden.
- Davidson, L., 2006, Evaluation of the SST-SAS Model: Chanel Flow, Asymmetric Difuser and Axi-Symmetric Hill, European Conference on Computational Fluid Dynamics, ECCOMAS CFD 2006.
- Maj. Christopher, A. Jones; Unmanned Aerial Vehicles (UAVs) an Assessment of historical operations and future possibilities; The research Department Air Command and staff College, 1997.
- Menter, F.R., Kuntz, M., Langtry, R., 2003, Ten Years of Industrial Experience with the SST Turbulence Model, Proceedings of the 4th International Symposium on Turbulence, Heat and Mass Transfer, pp. 625-632.
- Menter, F.R., 1992, Influence of Freestream Values on k-w Turbulence Model Predictions, AIAA Journal, Vol. 30, No. 6, pp. 1657-1659.
- Menter, F.R., 1994, Two-Equation Eddy-Viscosity Turbulence Models for Engineering Applications, AIAA Journal, Vol. 32, No 8, pp. 1598-1605.
- UIUC Airfoil Data Site, Michael Selig, Department of Aeronautical and Astronautical Engineering, University of Illinois at Urbana-Champaign, Urbana, Illinois 61801
<<http://www.ae.illinois.edu/m-selig/pd.html>> Accessed on: March 24, 2012.
- Zandonade, P.S.K., Rodrigues, J.L.A.F., Modelos Não-Lineares do Tensor de Reynolds na Simulação de Escoamentos Parietais.

8. RESPONSIBILITY NOTICE

The authors are the only responsible for the printed material included in this paper.